54

#### 1. Introduction

55 While clouds represent one of the largest modulators of Earth's radiation, with their impact 56 dependent on a variety of cloud physical and radiative properties, they remain one of the 57 more difficult components to represent in global climate models (Jiang et al. 2012). 58 Passive satellite observational datasets such as those from MODIS (Moderate Resolution 59 Imaging Spectroradiometer), AVHRR (Advanced Very High Resolution Radiometer). 60 HIRS (High-spectral Infrared Sounder), and ISCCP (International Satellite Cloud 61 Climatology Project) provide long-term, global cloud observations (Heidinger et al. 2013; 62 King et al. 2013; King et al. 2003; Rossow 1991; Rossow; Schiffer 1999; Wylie; Menzel 63 1999). However assessing the uncertainties in the cloud radiative properties retrieved by 64 these sensors has proved to be a complex and difficult task. Until recently, validation of 65 these retrievals was limited to ground and aircraft inter-comparisons. But with the 66 successful launch of CALIPSO (Cloud-Aerosol Lidar and Infrared Pathfinder Satellite 67 Observations) and CloudSat in April 2006 as part of the NASA-led Afternoon 68 Constellation (A-Train) (Stephens et al. 2002; Winker et al. 2010), researchers now have 69 access to a near-continuous global record of vertically resolved observations of cloud and aerosol properties with nearly coincident observations from MODIS Aqua Since launch. 70 the CALIPSO lidar (the Cloud Aerosol Lidar with Orthogonal Polarization, or CALIOP) 71 72 has proven to be a valuable tool for developing and evaluating passive cloud retrievals (Ackerman et al. 2008; Delanoë; Hogan 2010; Holz et al. 2008; Jint Nasiri 2013; Kahn et 73 74 al. 2007). CALIOP can directly measure cloud-top height with sensitivities that are an order of magnitude greater than the passive retrievals, while the CALIOP depolarization 75

P pauigneple

and attenuated backscatter measurements provide vertically resolved cloud phase discrimination (Hu et al. 2009) for cloud layers up to a cumulative optical depth of about 3.

Ice Optical Thickness (IOT) has also proved to be one of the more challenging properties to retrieve from space-based passive sensor measurement. In particular, it is quite difficult to infer the microphysical and radiative properties of optically thin upper tropospheric ice clouds (cirrus) from observations made by passive space-borne instruments due to the tenuous nature, extensive spatial scales, complex particle shapes, and a wide range of particle sizes. There is a pressing need to conduct independent validation to examine systematic biases between MODIS Collection 5 (C5) and CALIOP Version 3 (V3) retrievals of tenuous IOT (< 3.0). To this end, we use a month of collocated A-Train observation to compare the aforementioned retrieval products. A factor of two bias is found between MODIS and CALIOP unconstrained retrievals (presented in Figure 1), raising a major question regarding the utility of these data records to study ice cloud radiative processes. Here we seek to understand and resolve the CALIOP and MODIS IOT biases.

the ice particle scattering properties that relate the measured reflectance (MODIS) or attenuated backscatter (CALIOP) to the cloud's IOT and potentially the effective particle size. MODIS ice cloud forward radiative calculations in the visible/near-infrared (VNIR) depend directly on the ice particle phase function assumption, and to a first order on the associated asymmetry parameter (g). For CALIOP, an assumed extinction-to-backscatter ratio is required for so-called unconstrained retrievals where the algorithm is unable to make reliable estimates of cirrus IOT by measuring the attenuated backscatter coefficients

in some clear air region immediately below cloud base (Young and Vaughan, 2009).

Both MODIS and CALIOP IOT retrievals require a priori information concerning

introduce

Because solar background signals greatly reduce the signal-to-noise ratio (SNR) of the CALIOP daytime measurements, the vast majority of CALIOP daytime IOT estimates are derived from unconstrained retrievals. Uncertainties in the ice scattering property assumptions of either MODIS and/or CALIOP could account for the biases found in Fig. 1.

As will be discussed, an infrared (IR) cirrus IOT retrieval is relatively insensitive to ice particle size and scattering details compared to MODIS and CALIOP VNIR measurements, and thus provides an independent means to assess thin to moderately optically thick cirrus retrievals (IOT ~ 0–3). In addition, an IR retrieval provides radiative closure with solar reflectance based MODIS IOT retrievals in the sense that consistency in the two retrieved IOTs also implies forward model consistency with the respective top-of-atmosphere (TOA) VNIR and IR observations.

Using the NASA-funded SSEC Atmosphere Product Evaluation and Test Element (PEATE), now re-named the Suomi-NPP Atmosphere Science Investigator Processing System (SIPS), the sensitivity of MODIS retrievals to ice single scattering properties are investigated by repeated analyses of collocated January 2010 CALIOP and MODIS observations using a variety of ice crystal habits (Yang et al. 2012) and size distributions. Based on comparisons against IR retrievals, the MODIS MYD06 Collection 6 (C6) ice cloud optical property algorithm uses a single habit – severely roughened aggregated columns (Yang et al. 2012) – instead of the size-dependent multi-habit model (Baum et al. 2005) used for C5. The MYD06 C6 results also compare well with a new CALIOP version that uses a modified (larger) extinction-to-backscattering ratio for unconstrained IOT retrievals.

\* 51 ght confusion here regarding emphred consideration of CS/V3 at L84. I see man groups were merely starting what was "broken". But, just a word that I was confused, and that some text be added to better guide the reads to ward your hypothesis.

## 2. Ice Cloud Optical Thickness Retrieval Datasets

An overview of the relevant retrieval methodologies is presented here with a focus on the forward cloudy radiative transfer modeling assumptions and IR cirrus optical thickness

retrievals developed specifically for this study.

### 2.1 IR retrievals and radiative closure

122

125

126

127

128

129

130

131

132

133

The MODIS channel suite includes a range of IR channels extending well into the CO<sub>2</sub> absorption region (13-15 µm). The calibration of the IR channels has been extensively validated and proven to have high accuracy with uncertainties less than 0.5 K across a broad temperature range (Tobin et al. 2006). For cirrus, the IR radiative transfer is dominated by absorption, and thus is less complex than for the VNIR retrieval. In this section we discuss the IR radiative transfer methodology that is used both to retrieve the IR IOT as well as evaluate the MODIS and CALIOP retrievals.

134 The goal of radiative closure study is to relate the differences in the CALIOP and 135 MODIS retrieved IOT to the measured TOA channel radiance or Brightness Temperature 136 (BT) in the MODIS 11 μm channel. To calculate the TOA cloudy radiances requires an 137 accurate radiative transfer model, knowledge of the cloud boundaries, and well-138 characterized surface temperature/emissivity and atmospheric thermodynamic profiles. 139 LBLDIS (Turner et al. 2003), a cloudy radiative transfer model, is used for this analysis. 140 The model elegantly combines the clear sky Line By Line Radiative Transfer Model 141 (LBLRTM) (Clough; Moncet 1992) with the Discrete Ordinates Radiative Transfer 142 (DISORT) (Stamnes et al. 1988), a proven and accurate cloudy radiative transfer model. 143 The inputs required for LBLRTM are surface temperature and emissivity, vertically resolved temperature and water vapor profiles, and information regarding trace gas 144

145	concentrations such as CO <sub>2</sub> and O <sub>3</sub> . For this analysis, the surface temperature and
146	thermodynamic profiles are extracted from the NOAA Global Data Assimilation System
147	(GDAS) files that provide profiles at 1° spatial resolution every 6 hours. For each
148	MODIS and CALIOP field of view (FOV), the closest (in both time and space) GDAS
149	profile is selected. A fixed CO <sub>2</sub> concentration of 380 ppm and a climatological O <sub>3</sub> profile
150	is used. Given these inputs LBLRTM is run on the selected FOV filtered using the
151	collocated CALIOP V3 5km layer products (described in Section 3). The results of the
152	clear sky validation are discussed in Section 4
153	The cloud microphysics and thermodynamics are defined with a vertical
154	resolution of 500 meters within the cloud boundaries defined by the CALIOP layer
155	product. For example a cloud with a geometrical thickness of 1.5 km is divided into 3
156	layers with each layer defined by an optical thickness, effective radius and ice scattering
157	model. For example, for a cloud with a total optical thickness of 1.5 each layer will have
158	an optical thickness of 0.5. Using this methodology the vertical temperature profile is Significant Structure
159	accounted for in the radiative transfer. For daytime IR forward model calculations, the
160	effective radius from the MODIS optical property retrieval is used for all cloud layers.
161	For nighttime CALIOP comparisons, a fixed effective radius of 40 $\mu$ m is used in the IR
162	calculations.
163	The last remaining variable needed to calculate the TOA IR radiance is IOT.
164	LBLDIS is run independently using either the MODIS or CALIOP retrieved IOT,
165	resulting in high spectral resolution TOA radiances with the only differences being the
166	assumed IOT (i.e., MODIS or CALIOP). The spectrally resolved radiances are then
167	integrated over the MODIS Aqua 11 $\mu$ m channel (band 31) spectral response function

Are you constraining the CALIOP sample utall to limit the effects of attenuation and overestmetes of which cloud base height?

resulting in a simulated TOA radiance that can be directly compared to the measured MODIS 11  $\mu m$  observations.

In addition to LBLDIS spectral calculations, TOA longwave fluxes are calculated using the Rapid Radiative Transfer Model (RRTM) (Mlawer et al. 1997) that is also based on DISORT and LBLRTM and utilizes a correlated-*k* method for gas absorption along with broadband ice cloud parameterizations from (Fu et al. 2000). Identical inputs are used for RRTM and the LBLDIS TOA calculations with the only variable being IOT. The TOA fluxes are subsequently used to quantify the impact of the IOT biases on the global characterization of ice cloud radiative forcing.

IR observations provide the independent reference to understand differences between MODIS and CALIOP IOT retrievals. While radiance closure provides valuable information regarding TOA radiances and fluxes it does not provide a direct assessment of the individual CALIOP and MODIS IOT biases. To convert observed IR TOA radiance to IOT, two different retrieval approaches were used. First, we developed an IR window IOT retrieval that uses the collocated MODIS and CALIOP observations. This "reference" retrieval uses cloud boundary information from CALIOP coupled with the LBLDIS forward model and then retrieves the IR IOT using the MODIS 11 μm window channel observations that are coincident and collocated with CALIOP. A second method uses the spectral emissivity retrieved from the MODIS CO<sub>2</sub> emissive cloud-top pressure retrieval that is then related to the IOT and effective radius using a pre-computed lookup table (Heidinger et al. 2015). This method has the advantage of being computationally very efficient, not requiring the CALIOP cloud boundaries, and providing IOT for the entire MODIS swath. Both IR retrieval methods are discussed in more detail in the following sub-sections.

# 2.1.1. Combined MODIS IR Window and CALIOP Retrievals

A single channel IR window IOT retrieval was developed for this study using combined CALIOP and MODIS observations and the LBLDIS forward radiative transfer modeling discussed in the previous section. The method constrains the cloud boundaries using the collocated CALIOP 5km layer products and uses surface and atmospheric temperatures information from GDAS. TOA radiances are simulated using LBLDIS with IOT retrieved by minimizing the measured MODIS channel 31 (11 μm) and calculated BT differences. The retrieval assumes the cloud extinction is evenly distributed in the vertical throughout the cloud. This simplification has the potential to bias the HOT for FOV where the IOT is distributed non-uniformly in the vertical (Maestri; Holz 2009). The cloud geometric km to reduce 101...

Ly Makes me word even

Sorther about

attenuation

and resolving

claid base thickness is thus limited to no greater than 4 km to reduce IOT biases that can be introduced by non-homogeneous layers.

# 2.1.2. MODIS IR Spectral Emissivity Retrievals

The MODIS C6 CO<sub>2</sub> slicing algorithm provides retrieved spectral emissivity for the 8.5, 11, and 12 µm channels (channels 29, 31, 32) that have sensitivity to both the IOT and effective radius. As described in (Parol et al. 1991),  $\beta$  ratios can be approximated based on these emissivities and are related to the asymmetry parameter (g), single-scattering albedo ( $\omega_0$ ), and extinction efficiency ( $Q_e$ ) as follows:

210

192

193

194

195

196

197

198

199

200

201

202

203

204

205

206

207

208

209

211 (1) 
$$\beta_{\lambda_1\lambda_2} = \frac{Q_{e,\lambda_1}(1-\omega_{o,\lambda_1}g_{\lambda_1})}{Q_{e,\lambda_2}(1-\omega_{o,\lambda_2}g_{\lambda_2})}$$

Thus  $\beta$  is the ratio of the scaled absorption extinction in two spectral channels ( $\lambda_1$  and  $\lambda_2$ ).

The effective radius is first retrieved by matching simulated ice single-scattering calculations of g(r),  $\omega_0(r)$ , and  $Q_e(r)$ , each integrated over the appropriate MODIS spectral response functions, to the retrieved MODIS  $\beta$  ratios. For this analysis the scattering properties of severely roughened aggregated columns (Yang et al. 2012) are used to be consistent with the MODIS C6 cloud optical property retrievals.

Using the effective radius to define g(r),  $\omega_0(r)$ , and  $Q_e(r)$ , the extinction optical thickness is then retrieved by relating the 11  $\mu$ m emissivity to the extinction optical thickness in the form ((Van de Hulst 1974))

222 (2) 
$$\tau_{vis} = \frac{2}{Q_e} \left( \frac{\tau_{abs}}{(1 - \omega_o g)} \right),.$$

where  $\tau_{abs}$  is the IR absorption optical thickness and  $\tau_{vis}$  is the extinction optical thickness at 532 nm. This derivation assumes that the ratio between the absorption and extinction optical thickness is a factor of 2 in the IR. Based on ice cloud single-scattering calculations (Yang et al. 2012) and assuming that the majority of ice clouds have an effective radius greater than 10  $\mu$ m, this assumption is expected to have introduce no more than 10% uncertainty. (Heidinger et al. 2015) provides a more detailed discussion of the retrieval methodology. This approach can be applied without the need for the CALIOP cloud boundaries, and provides full swath IR IOT retrievals. We leverage this capability to investigate the MODIS IOT retrieval biases as a function of view angle.

### 2.2 CALIOP Ice Cloud Optical Thickness Retrievals

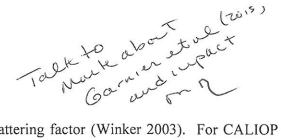
CALIOP is a two wavelength elastic backscatter lidar that measures attenuated backscatter components polarized parallel and perpendicular to the transmitted laser light

at 532 nm and total attenuated backscatter at 1064 nm (Hunt et al. 2009). Once the received signals have been background-subtracted and calibrated (Powell et al. 2009), a tightly integrated suite of retrieval algorithms is used to detect layer boundaries (Vaughan et al. 2009) and classify layers as either clouds or aerosols (Liu et al. 2009). Layers classified as clouds are further classified according to thermodynamic phase as either ice clouds or water clouds (Hu et al. 2009). Layer optical thickness (including IOT) is then retrieved using one of two techniques: constrained or unconstrained retrievals (Young; Vaughan 2009). Constrained retrievals are applied whenever the effective two-way transmittance of a layer,

245 (3) 
$$T_{eff}^{2} = exp(-2\eta\tau) = \exp\left(-2\eta \int_{layer\ top}^{layer\ base} \sigma_{c}(r)dr\right)$$

can be directly and reliably measured. In this expression,  $\tau$  is the layer optical depth (IOT for ice clouds),  $\sigma_c(r)$  is the range-resolved cloud extinction coefficient, and  $\eta$  is a multiple scattering correction factor whose value depends on the lidar sensing geometry and the scattering characteristics of the particulates being measured. While  $T_{eff}^2$  estimates can be obtained from measurements of clear air, opaque water clouds, and ocean surfaces (see [Josset et al. 2012; Yongxiang et al. 2007; Young 1995], respectively), the CALIOP V3 algorithm only implements the clear air technique, in which  $T_{eff}^2$  can be obtained directly from the ratio of the mean attenuated scattering ratios calculated in regions of clear air located immediately above cloud top and below cloud base (Vaughan et al. 2005). Retrieving IOT from measurements of  $T_{eff}^2$  requires knowledge of the appropriate

ordu-



multiple scattering factor (Winker 2003). For CALIOP measurements of cirrus clouds, (Josset et al. 2012) determined the mean multiple scattering factor to be  $0.61 \pm 0.15$ . In the CALIOP V3 algorithm,  $\eta$  is fixed at 0.6 for all cirrus clouds.

Constrained retrievals are the preferred method for retrieving IOT from CALIOP measurements. However, because solar background light significantly degrades the CALIOP SNR during daylight operations, V3 constrained retrievals occur almost exclusively during nighttime observations, thus severely limiting direct comparisons with MODIS IOT retrievals derived from VNIR solar reflectance. For the vast majority of daytime observations, CALIOP IOT retrievals use an unconstrained technique that requires *a priori* knowledge of the cirrus extinction-to-backscatter ratio (i.e., lidar ratio),

$$S_c = \frac{\sigma_c(r)}{\beta_c(r)},$$

where  $\sigma_c(r)$  and  $\beta_c(r)$  are, respectively, the cloud extinction and backscatter coefficients. IOT is then obtained by solving the lidar equation using specified values of  $\eta$  and  $S_c$ (Young; Vaughan 2009). Note that while the cloud extinction and backscatter coefficients are explicitly range-dependent, their ratio is assumed to be range-invariant. Although Sc for cirrus most likely varies depending on crystal habit and size distribution, the CALIOP V3 unconstrained retrievals use a globally constant default value of  $S_c$  = 25  $\pm$  10 sr. This value was determined prior to launch from the best information available from numerous ground-based and airborne data sets (e.g., Holz 2002; Sassen 2001; Yorks et al. 2011). 

Errors in lidar ratio selection for unconstrained retrievals generate corresponding errors in the resultant estimates of IOT. In particular, an underestimate of  $S_c$  will result in CALIOP underestimating IOT. The selection of the default CALIOP lidar ratio is thus one of the potential major sources of bias in the CALIOP unconstrained retrievals that

can be investigated using IR observations from either MODIS or the CALIPSO IIR (Imaging Infrared Radiometer) instrument (Garnier et al. 2015).

### 2.4 MODIS Ice Cloud Optical Thickness Retrievals

The MODIS imager provides measurements in 36 spectral channels, covering the Visible Near Infrared (VNIR), Shortwave Infrared (SWIR), Midwave Infrared (MWIR), and thermal IR portions of the spectrum. Spatial resolution is 250 m in two VNIR channels, 500 m in 5 VIS/SWIR channels, and 1 km in the remaining channels.

The MODIS cloud optical/microphysical property algorithm is used to generate a single cloud product designated by the NASA Earth science data type (ESDT) names MOD06 and MYD06 for Terra and Aqua MODIS, respectively (hereafter referred to as MYD06 since the algorithms are essentially identical and this study is focused on MODIS Aqua observations). For daytime measurements, the 1 km cloud retrieval algorithm uses multiple spectral channels (primarily six VNIR, SWIR and MWIR channels, as well as several thermal channels) to simultaneously retrieve cloud optical thickness, effective radius (and derived water path) and thermodynamic phase for liquid and ice phase clouds. In addition to the 1 km MODIS Level-1B calibrated radiance product, the algorithm requires the following input: MODIS cloud mask (MYD35) including 250 m mask information (Ackerman et al., 1998), the cloud-top pressure portion of MYD06 (Ackerman et al. 2008; Holz et al. 2008), and a variety of ancillary datasets. Heritage algorithm work is discussed in King et al. (2003) Nakajima; King (1990) Platnick; Twomey (1994) Platnick et al. (2001); Platnick et al. 2003)

distinct layers in cases where the base of the upper layer is separated from the top of the lower layer by as little as a single range bin (60m). For a passive retrieval such as from MODIS, a 60 m vertical separation will have little impact on the retrieval results, assuming both layers are ice. To improve the comparison yield, and provide a more representative distribution of single layer ice clouds for inter-comparing the passive observations, CALIOP 5 km ice cloud layers with a vertical separation of 3 km or less are merged to form single, vertically contiguous layers. The CALIOP extinction profile is then integrated for each profile using the redefined layer boundaries, thus providing an aggregated IOT. Ice clouds with total geometrical thickness greater than 4 km using this single layer definition are excluded from the comparison.

The MODIS IOT retrievals are filtered using the C5 MODIS Quality Assurance (QA) parameters and a horizontal heterogeneity threshold. MODIS IOT retrievals (i.e., with the QA usefulness flag set to 1 and the QA confidence flag set to 3) are used in the comparison. Using this filtering provides the highest quality MODIS retrievals and removes all cloud edges from the comparison. To reduce uncertainties resulting from spatial sampling differences between MODIS and CALIOP, the standard deviation of a 5x5 pixel box centered over the collocated pixel is computed. Only collocated pixels where the MODIS IOT standard deviation is less than 0.5 are used; we find, however, that the comparison results are relatively insensitive to this threshold.

Figure 1 reveals a systematic bias between the MODIS and CALIOP IOT's, with MODIS approximately a factor of two larger than the CALIOP unconstrained retrievals. An independent methodology is needed to assess this difference since both retrievals depend on ice scattering property assumptions. As discussed in the methodology section, the IR observations provide sensitivity to the IOT given well-constrained cloud

boundaries with uncertainties that are independent of the CALIOP and MODIS VNIR retrievals. Spectrally resolved TOA radiances are calculated for the three different retrieval methods - MODIS, CALIOP unconstrained (daytime measurements), and CALIOP constrained (nighttime measurements) - using LBLRTM and LBLDIS. All three calculations use identical cloud boundaries defined by the merged CALIOP 5 km layer heights and the same thermodynamic profiles and ocean surface temperatures (GDAS), with the only difference being the IOT used in the calculation. The spectrally resolved TOA radiances are then integrated over the MODIS channel 31 (11 µm) spectral response function. To investigate the accuracy of the combined GDAS and TOA clear collowtus sky LBLRTM calculations, simulated TOA 11 µm BT for clear sky FOV's identified using both the MODIS and CALIOP cloud masks were compared to the measured MODIS 11 µm channel BTs. The mean bias between the simulated and observed BT is less than 0.2 K, which is within the expected calibration uncertainty of MODIS (Tobin et al. 2006). Figure 2a presents the MODIS C5 and CALIOP V3 BT closure results. The figure

374

375

376

377

378

379

380

381

382

383

384

385

386

387

388

389

390

391

392

393

394

395

396

397

Figure 2a presents the MODIS C5 and CALIOP V3 BT closure results. The figure reveals a sobering finding which is that neither the MODIS C5 nor the CALIOP V3 unconstrained IOT retrievals provide radiative closure in the window IR. Furthermore, the respective retrievals are biased in opposite directions. For MODIS C5, the calculated TOA BT is colder than the measured BT with a mean bias of -8.7K, implying the MODIS IOT is on average biased high. In contrast, the TOA BT calculated using the CALIOP V3 unconstrained IOT has a mean bias of +12.1 K, suggesting the CALIOP retrieval is biased low. The CALIOP V3 constrained retrievals, which do not require an assumed lidar ratio but only an estimate of the multiple scattering correction, demonstrate much better agreement with a mean bias of +1.4 K.

\* I sut this result; then, consistent with what you'd expect within the context of your available you'd expect within the context of your available obs? modes is 137's are under constrained whrespect to differ about top elements, which you're directly to differ hed via CALIOF (= warmbian) CALIOF detection.

To put the biases into a radiative context, the cloudy IR TOA fluxes are computed JCBH 398 for each collocated FOV using RRTM. The calculations use the CALIOP cloud is 4 boundaries, the surface and atmospheric profiles from GDAS, and the MODIS retrieved effective radius. For each collocated FOV two RRTM calculations are computed with the 402 only difference being the IOT used (MODIS or CALIOP) with the results presented in 403 Figure 2b. The mean TOA flux difference between MODIS and CALIOP unconstrained retrievals is +23 W m<sup>-2</sup> with a standard deviation of 21 W m<sup>-2</sup>. For the tenuous cirrus being 404 contrast between the surface and the mean emitting temperature of the cloud. The very petroocquare differences in the wings of the distribution in Fig. 1b occur primarily near the investigated, the sensitivity of the TOA flux to IOT is primarily driven by the thermal 405 406 407 tropics where the thermal contrast is greatest between the cloud and the surface. For this 408

# 5. IR Retrievals as a Reference Optical Thickness

region TOA differences as large as 50 W m<sup>-2</sup> are found in Figure 2b.

399

400

401

409

410

411

412

413

414

415

416

417

418

419

420

Because the sensitivity of IR IOT retrievals to ice crystal habit selection is minimal, these retrievals provide an independent means to evaluate the CALIOP and MODIS solar reflectance retrievals. As discussed in Sect. 2, the main sources of uncertainty in the IR IOT originate from characterizing the surface temperature and having an accurate determination of the cloud emitting temperature. To reduce the surface temperature uncertainty, the results of this section are restricted to non-polar (± 60 degrees) oceanonly cases.

The comparisons with IR window IOT retrievals shown in Figure 3 reveal biases in both the MODIS (a) and daytime CALIOP unconstrained (b) retrievals (high and low, respectively) that are consistent with the radiative closure results presented in Figure 2.

The magnitude of the bias relative to the IR is approximately +40% for MODIS. For CALIOP there is a non-linear dependence between the IOT and the negative bias relative to the IR, with the bias increasing substantially for IR IOTs greater than unity; the CALIOP results are discussed further in Section 5.2.

421

422

423

424

425

426

427

428

429

430

431

432

433

434

435

436

437

438

439

440

441

442

443

444

attematic

A limitation of the IR window IOT data set is that only a small subset of the MODIS across track swath can be assessed due to the very close coordination between 7 the MODIS and CALIOP orbits. To investigate MODIS IOT scan angle dependencies we use the MODIS spectral IR IOT retrieval described in Sect. 2.1.2. Figure 4a shows the MODIS C5 liquid (warm colors) and ice (cool colors) phase cloud optical thickness for an example MODIS data granule (January 11 2010, 06:25 UTC). Fig. 4b presents the histogram of the ratio between the MODIS IOT and the full swath IR IOT (described in section 2.1.2) separated by viewing angle ranges as indicated by the colored lines overlaid on the IOT image. A ratio of unity would suggest good agreement between the spectral IR and VNIR IOT retrievals. However, as illustrated in the following section, for the MODIS C5 retrievals (solid lines) the modes of the distributions vary with scan angle, and the bias is seen to be an increasing as a function of scan angle. This is an important result, as it demonstrates necessity that this scattering angle dependence can provide an additional constraint on ice radiative model selection. In addition, because CALIPSO and Aqua have similar orbits, only a small range of MODIS viewing angles are included in the collocated inter-comparison, thus the possible strong dependence on viewing angle implies the collocated analysis is representative only of the view angle ranges sampled. Finally, given the lack of significant scattering in the IR, the scan dependent bias further suggests the issue is with the MODIS C5 VNIR retrievals. This is investigated in the next section.

Be Does 13T Show some bras? If so, does this supply relate to "effective"! FOT relative to Satellite FOV that inglieucus your I'R

#### 5.1 Ice Radiative Model Sensitivities in MODIS

Though a primary focus of this investigation is on optimizing C6 ice models to improve IOT intercomparisons, it is understood that ice model crystal habits also affect the particle single scattering albedo retrieved using the SWIR and MWIR channels that provide effective particle size information. Figure 5a and Figure 5b show the 2.13  $\mu$ m and 3.7  $\mu$ m channel co-albedo, respectively, as a function of Cloud Effective Radius (CER) for four habit realizations, namely the C5 habit mixture (black line) and the three severely roughened habits solid aggregate plates (green line), solid bullet rosettes (red line), and aggregate columns (blue line). To the extent that CER retrievals of an asymptotically thick cloud in the SWIR/MWIR are essentially a retrieval of co-albedo, the difference between the aggregated column and C5 model co-albedo implies an effective radius difference of +2  $\mu$ m and -8  $\mu$ m at the 2.1  $\mu$ m and 3.7  $\mu$ m wavelengths, respectively, for a C5 effective radius of about 35  $\mu$ m; smaller C5 retrieved sizes would result in larger differences.

Figure 6 shows the asymmetry parameter sensitivity to habit for the same four habits shown in Figure 5. Evidently, the habit-sensitivity of the asymmetry parameter is also strong in both the 2.1 µm and 3.7 µm MODIS channels. While the asymmetry parameters of three severely roughened habits are not constant with effective size (though at 2.1 µm the aggregate plates and aggregate columns are nearly constant), the C5 model has much larger size sensitivity at both wavelengths. Aggregated columns, with smaller asymmetry parameters relative to C5, will result in a larger retrieved CER estimates. This is because the resulting increase in modeled SWIR reflectance for a given effective size causes the measured reflectance to be associated with a more absorbing (i.e., larger)

particle. Therefore, the effect of both co-albedo and asymmetry parameter differences between the severely aggregated column habit and the C5 model act to increase retrieved effective radii at 2.1 µm, while at 3.7 µm some cancellation of effects can be expected.

The single habit radiative models shown in Figure 5 and Figure 6 are used to build look-up tables that were integrated into the MODIS C6 cloud retrieval development code. A month of data was processed for each habit. It was found that the habit that provided the best consistency with the IR window retrievals (Sect. 2.1.1) is the severely roughened aggregated column model. The IOT retrieval comparison with the IR window retrievals using this model is shown in Figure 7a, where the MODIS reflectance-based retrievals using the severely roughened aggregated column model are now clustered around the 1-to-1 line. In addition, this aggregated column model was used to assess the MODIS retrieval swath dependence previously shown in Figure 4b. The improvement of the aggregated column model (dashed lines) relative to the C5 model (solid lines) is significant. Both results led to the decision to use the severely roughened aggregated column radiative model for the MODIS C6 cloud optical/microphysical property retrievals.

Figure 8 shows an example of ice cloud retrievals for C5 and C6 for typhoon Fung-Wong. The typhoon was located south of Taiwan at the time of the MODIS Aqua data granule acquisition on September 20, 2014 (0530 UTC). The C5 and C6 ice (cool colors) and liquid (warm colors) cloud optical thickness retrievals are shown in the middle and right panels, respectively. In addition to ice radiative model differences, MYD06 C5 and C6 have different schemes for the cloud thermodynamic phase yielding different ice and liquid phase pixel populations, though the optical thickness spatial patterns are similar for regions having the same phase. Because of the different phase

assignments made by these two scheme, quantifying ice model retrieval sensitivities requires the comparisons be restricted to only those pixels for which both algorithms generate successful retrievals that identify identical cloud phases. With this pixel filtering, the left panel of Figure 8b shows the normalized IOT distribution for the optical thickness range of the plot. The C6 IOT mode is roughly 27% smaller than the C5 mode, while the mean is decreased by about 15%, from 4.16 for C5 to 3.55 for C6. The 2.1  $\mu$ m ice cloud effective particle radius retrievals are shown in the right panel, with the C6 mode and mean both increasing by about 4  $\mu$ m (+15%) for C6 relative to C5.

### 5.2 MODIS C6 model selection methodology

492

493

494

495

496

497

498

499

500

501

502

503

504

505

506

507

508

509

510

511

512

513

514

515

The MODIS IOT retrieval depends strongly on assumed ice scattering properties that are needed to relate the measured reflectance to the retrieved IOT. The MODIS C5 retrieval used empirically derived habit and size distributions with asymmetry parameters ranging between 0.79 and 0.88, depending on the ice cloud effective radius (Baum et al., 2005). By conducting an infrared closure analysis, we have shown that the C5 parameterization is not representative of the globally averaged ice scattering properties. More recent investigations of the ice cloud asymmetry parameter suggest that most ice REFSI clouds have values around 0.75 in the visible spectrum. Additionally, use of the C5 ice cloud radiative model results in MODIS retrieval biases are strongly dependent on the viewing angle, as demonstrated in Figure 4. These findings motivated the investigation of new ice scattering models that have lower asymmetry parameters and weaker dependence on ice effective radius/Since the MODIS C5 algorithms were finalized, new ice scattering models that incorporate roughened ice crystal parameterizations have been developed (Yang et al. 2012). Experimentation with these new models demonstrates that a modified gamma distribution of severely roughened aggregated columns provides a significantly

lower visible asymmetry parameter ( $\sim 0.75$ ) that shows very little dependence on ice	
effective radius. For testing purposes, the MODIS cloud retrieval algorithm team	
implemented these new scattering properties in the MYD06 retrieval algorithm. The	
updated algorithm was then run on the Atmospheric PEATE and the resulting data was	
collocated with CALIOP measurements. Simulated TOA cloudy MODIS 11 $\mu m$ brightness	
temperatures (BT) are then computed using the reprocessed MODIS IOT retrievals and are	
compared to the MODIS measured BT, These new results presented in Figure 10b//The	
updated ice scattering models generate greatly improved IOT estimates that show very	
close to a one-to-one correspondence with the independently derived IR IOT values	
(Figure 7a). Additionally the view angle dependent bias is largely removed, as presented in	
Figure 4c. Based on these results, the recently reprocessed MODIS C6 cloud	
optical/microphysical property product (now in forward production) uses a modified	
gamma distribution consisting of a single habit of severely roughened aggregated columns	
for ice cloud retrievals. An additional benefit of the single habit is that it simplifies the	
retrieval and increases the reproducibility of the scattering properties by the research	
community. There is no Fig. 42??	

Figure 10a presents the same filtered 2-D histogram comparing CALIOP and MODIS as Figure 1 but using the ice radiative model modifications made for MODIS and the updated lidar ratio (32 sr) for CALIOP. Figure 10b presents the IR radiative closure for the update IOT retrievals for January 2010. Notice the large bias between the MODIS and CALIOP un-constrained IOT is significantly reduced and the IR radiative closure shows very good agreement for all three IOT retrievals. There is still a tendency for the MODIS IOT to be larger than CALIOP in Figure 10a. The MODIS C6 IR closure in Figure 10b

?? where ded this comes on next page? Octobu? Comeson? page? Octobu? U. Static N. how in this carninetal (2015)?

also demonstrates this bias, with the tail of the distribution weighted to negative BT differences suggesting the remaining bias is specific to MODIS.

### 5.3 Ice Lidar Ratio Sensitivities in CALIOP

As previously discussed, CALIOP uses one of two methods, i.e., constrained and unconstrained to retrieve IOT. The constrained method requires high SNR in clear air regions immediately above and below the cloud. This SNR requirement limits the constrained retrieval primarily to nighttime FOVs, because solar background light severely degrades the clear air SNR during the daytime. This precludes direct comparison of the constrained retrievals with the MODIS daytime optical property retrievals. The IR retrieval, being day/night independent, allows for direct inter-comparisons between the MODIS IR IOT retrievals and both the constrained and un-constrained CALIOP IOT retrievals providing a means to evaluate the two retrieval methods against a consistent reference.

Figure 3b presents the joint histogram between the unconstrained CALIOP and the MODIS window IR IOT for January 2010 for single layer cirrus. The filtering criteria are the same as in Figure 1, except both day and night observations are included. The CALIOP layer optical thickness is filtered using the extinction quality control (QC) flags provided as part of the L2 products. Only QC values of 0 (unconstrained solution, no lidar ratio adjustment), 2 (unconstrained solution, lidar ratio decreased) and 4 (unconstrained solution, lidar ratio increased) were selected. Consistent with the findings of (Garnier et al. 2015), Figure 3b shows CALIOP unconstrained IOT is significantly low-biased with respect to the IR IOT, with a non-linear dependence as a function of

IOT. Figure 9 compares the CALIOP constrained retrievals (QC=1) to the MODIS IR COT for the same filtering criteria. This comparison reveals a distinct difference between the CALIOP constrained and unconstrained retrievals (Figure 3b), as the constrained retrievals demonstrate a significantly smaller bias relative to the IR IOT. While the CALIOP IOT retrieval requires estimates of the multiple scattering contributions for both the constrained and unconstrained retrievals, the un-constrained method also requires an assumed lidar ratio whereas the constrained retrieval does not. Because both retrievals use an identical fixed multiple scattering factors, the difference between the constrained and unconstrained retrievals relative to the IR can be attributed to the use of an assumed lidar ratio in the unconstrained retrieval.

To investigate the sensitivity of the CALIOP IOT retrievals to the lidar ratio, a month of CALIOP L2 products was processed (January 2010) with the default lidar ratio increased to 32 sr. This revised value is the mean of all V3 constrained solutions of randomly oriented ice clouds (3,091,952 cases) measured between 28 November 2007 (when CALIPSO permanently changed its pointing angle to 3° off nadir) and 30 June 2012. It is important to note that the selection of this new default lidar ratio was based on ongoing quality assurance analyses conducted by the CALIOP algorithm team that were wholly independent of the IR inter-comparisons. The modified CALIOP product was ingested by the Atmospheric PEATE and collocated with both the MODIS C5 and C6 products and the MODIS IR retrievals. The modified CALIOP unconstrained retrievals compared to the reference IR IOT is presented in Figure 7b. Compared to the standard V3 products (Figure 3b) the change in the lidar ratio significantly reduced the bias compared to IR IOT, and the non-linear behavior at large IOT is almost completely removed. This is because optical depth is a nonlinear function of lidar ratio, thus weakly scattering

layers show minimal changes in IOT while the changes in strongly scattering layers are much more substantial. This result strongly suggests that the current V3 unconstrained lidar ratio of 25 sr should be increased in future versions of the CALIOP data products.

586

587

588

Arent Just de thought

# 6. Conclusions

The MODIS Collection 5 (C5) ice optical thickness (IOT) retrievals are compared to the

Version 3 (V3) CALIOP IOT for one month (January 2010) of collocated single layer ice

clouds. The comparison reveals a factor of two differences between the retrievals as

presented in Figure 1. Using IR observations from MODIS as an independent means of

assessing the CALIOP and MODIS IOT clearly demonstrates that both retrievals have

significant biases, but in opposite directions: MODIS C5 systematically overestimates IOT

while CALIOP V3 systematically underestimates IOT.

The decision to use the single severely roughened aggregate column habit as the MODIS C6 ice cloud radiative model was made solely to achieve closure with IR retrievals in a global sense. Our use of this model for this purpose does not imply that it is a suitable microphysical model for use in understanding ice particle physical processes, e.g., size distribution evolution, fall speed distribution, etc. Furthermore, the IR comparisons were done in conjunction with collocated CALIOP observations that that allow for the filtering of multi-layer ice phase clouds from the statistical study; The data set used here is clearly a subset of actual scenes and so may not be reflective of the full distribution of ice clouds observed by the sensors. Finally, it is recognized that using a fixed ice radiative model for global retrievals is only meaningful in a climatological sense and may be expected to breakdown in instantaneous and/or regional studies.

The severely roughened aggregated column model adopted for the MODIS C6 ice cloud algorithm has a fixed aspect ratio with an asymmetry parameter of about 0.75 in the visible for all effective sizes. This produces results that are quite consistent with those generated using the Inhomogeneous Hexagonal Mono-crystal (IHM) model derived by (C.-Labonnote et al. 2001 asymmetry parameter of about 0.77) that provided a good

match with observed POLDER view angle-dependent VNIR reflectance. Other studies have also suggested that featureless (i.e., smooth) phase functions indicative of roughened or highly asymmetric aggregated habits with relatively small asymmetry parameters are needed to match aircraft and satellite observations e.g., (Baran et al. 2001; C. -Labonnote et al. 2000; van Diedenhoven et al. 2013).

613

614

615

616

617

618

619

620

621

622

623

624

625

626

627

628

629

630

631

632

633

634

635

636

The Generalized Habit Model (GHM) (Baum et al. 2010) was also tested but did not the same level of radiative closure with the IR IOT retrievals compared to the severely roughened aggregated columns (comparison shown in Fig. 7a). While there was an improvement with respect to the C5 ice model (comparison shown in Fig. 3a), the GHM model resulted in IOT retrievals that were still significantly larger than the IR because of larger asymmetry parameters in the visible relative to the severely roughened aggregated column model (about 0.77 at an effective radius of 5 μm up to 0.82 at 60 μm). (Cole et al. 2012) also tested the GHM as well as single habit models from (Yang et al. 2012) and (Yang et al. 2003) against POLDER polarized and total reflectance observations across a range of scattering angles/Polarized angular observations agreed well with a severely roughened version of the GHM. However, it was concluded that there was no single habit/model that is best in all respects for the reflectance (derived spherical albedo) consistency tests, though the severely roughened aggregated column model was not included in the analysis. Similarly, (Baran; Labonnote 2007) also noted that though the IHM model provided good consistency with POLDER directional reflectance distributions, it was less successful in matching the angular distribution of polarized reflectances. Due to vertical size stratification in ice clouds it is possible that different models are needed to match polarized observations (weighted towards the uppermost portion of the cloud-top) with total reflectance observations (weighted deeper

into the cloud), e.g., (Platnick 2000) and (Zhang et al. 2010) Given that MODIS retrievals are based on total reflectance, it is expected that directional reflectance consistency with POLDER is the more relevant metric. Further, the study of (Zhang et al. 2010) shows there is little difference between IOT retrieved from reflectance and IR observations for the model case study considered. (Fauchez et al. 2014) demonstrated that for 1km IR observations, sensitivities to 3-D effects are limited to horizontal heterogeneity (plane-parallel approximation or PPA bias) and the effect of vertical heterogeneity is small. Though more extensive heterogeneity studies are needed, these studies do suggest the utility of using IR IOT retrievals to assess MODIS reflectance-based ice radiative models. Finally, we note that recent comparisons have demonstrated consistency between Aqua MODIS C6 IOT retrievals and those from AIRS Version 6 (Kahn 2015).

For CALIOP it is found that the bias relative to the IR for the V3 IOT retrievals depends on the retrieval method used. While CALIOP can make direct measurements of the effective two-way transmittance of the layer, the retrieved optical thickness depends only on an estimate of the multiple scattering factor and the accuracy of the molecular attenuated backscatter profile (calculated from a temperature and pressure profile using Rayleigh scattering theory). However, daytime solar background noise limits the applicability of this constrained retrieval technique to mostly nighttime observations, thus prohibiting direct comparisons to the MODIS daytime optical retrievals. For the constrained retrieval we find good agreement with the IR radiative closure (Figure 2) and the IR IOT in Figure 9. However, the majority of the daytime CALIOP retrievals use the unconstrained method that requires an *a priori* specification of the cloud extinction-to-backscatter ratio. It is these unconstrained retrievals that are directly compared to the

MODIS C5 IOT in Figure 1 and to the IR in Figure 2 and Figure 3. The CALIOP V3 unconstrained IOT retrievals show a significant low bias relative to both the IR and the constrained CALIOP retrievals. Since both CALIOP methods assume an identical multiple scattering correction, this suggests that the default lidar ratio (25 sr) used in the V3 CALIOP unconstrained retrievals is too low. As part of this investigation the CALIOP algorithm team processed a month of retrievals using a lidar ratio of 32 sr for the unconstrained retrievals with results presented in Figure 7b. It is important to note that the selection of a lidar ratio of 32 sr was not based on the IR inter-comparison studies, but instead was derived from independent analyses of the nighttime constrained retrievals conducted by the CALIOP algorithm team in order to improve the accuracy of the CALIOP unconstrained retrievals and increase the consistency of IOTs reported by the constrained and unconstrained retrievals.

### 674 Acknowledgements

- We would like to acknowledge the NASA University of Wisconsin Atmospheric
- 676 PEATE/SIPS that provide the processing and data accessed needed to conduct this
- 677 research. We would also like to thank the CALIOP and MODIS algorithm teams for their
- 678 support. This research was funded by NASA grant NNX15AG12G and NASA Langley
- 679 Contract SSAI Task A-014 E-001D.

### **Bibliography**